

We thank the Reviewer for the constructive comments and suggestions. In the following we provide a detailed response to each point. The Reviewer’s comments are in blue text, while our replies are black.

This work investigates the control of avulsions in bifurcated channel systems; a main channel splitting into 2 equal sub channels. Towards this end, the authors build a mathematical/numerical model, extending the well known analysis presented by Bolla Pittaluga et al. (2003) (BRT). The proposed model can track the evolution of a perturbation at the branching point of the sub-channels. In the first place, the model recovers the regimes identified in BRT. At low channel aspect ratios, following a perturbation, the system recovers balanced flows in each of the sub-channels. Beyond a critical aspect ratio Beta_c , however, the long term equilibrium of the flow in the system is unbalanced. This work show that as the aspect ratio is increased further, a second threshold Beta_TH is reached, here the sub channel, with the least flow, exhibits a partial-avulsion—where the channel still carries flow but ceases to transport sediment. Depending on the length of the sub channels, as the aspect ratio is increased even further, a point is reached where full avulsion occurs, i.e. the channel does not convey either water or sediment.

1. I think that the analysis in this paper is of sufficient interest to stand alone but also feel that it would be significantly enhanced, if the authors can point toward experimental or field evidence of the behaviors predicted by the math. For example, referring to Figure (9), it appears, by my calculations, that full avulsion would be reached in a system with channels of water depth of 2 m, width 40 m, and length 1 km+. How common are such conditions in field settings? (eg. Wax Lake in Louisiana)? Are records of permanently avulsed channels seen in such systems? Are records of permanently avulsed channels seen in field systems with shorter channel lengths and smaller aspect ratios?

We thank the Reviewer for the suggestions. Unfortunately, the available datasets are not sufficient to allow a detailed verification of model results.

Data from physical models are scarce, and experiments were mainly focused on the analysis of the effect of specific “forcing” factors. For example, the laboratory experiments by Salter et al. (2019) were tailored to depositional environments and reproduced bifurcations with prograding branches, while Szewczyk et al. (2020) analysed the influence on water discharge partition of changing the bifurcation angle, for values of the aspect ratio β_0 much smaller than

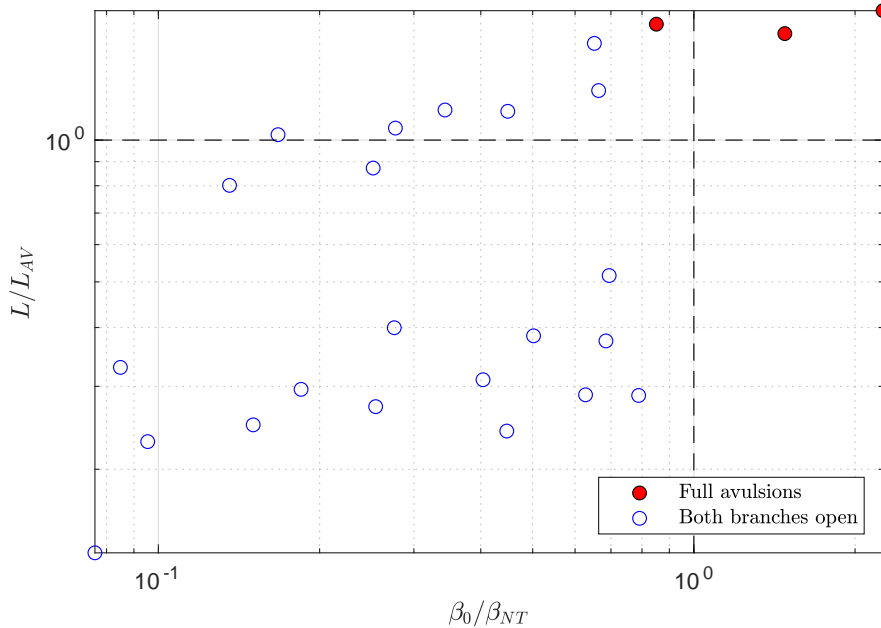


Figure AC1: Results from the analysis of experimental data by Bertoldi and Tubino (2007). Consistently with our theory, experiments where full avulsions were observed (filled markers) fall in the region $\beta_0 > \beta_{NT}$ and $L > L_{AV}$.

the no-transport threshold β_{NT} . To the authors' knowledge, the laboratory experiments by Bertoldi and Tubino (2007) are the only ones that analyse how initially balanced “free” bifurcations develop unbalanced configurations, possibly leading to partial or full avulsion. Indeed, a specific analysis of their results seem to support our findings, as shown in Figure AC1 where we report, for each experimental run, the computed values of β_0/β_{NT} and L/L_{AV} . Consistently with our predictions, they reveal that full avulsions (i.e. the complete closure of one of the branches) were observed in the three experimental runs in which β_0 was greater than (or closer to) β_{NT} and the channel length L was longer than the avulsion length L_{AV} .

Further support to our findings is also provided by the results of Ragno et al. (2022) who analysed nearly 200 bifurcation-confluence units of sand-bed and gravel-bed rivers. They found that field data show the existence of quasi-universal relations for the branches length when scaled with bankfull variables of the main upstream channel (the mean depth or width). The resulting average dimen-

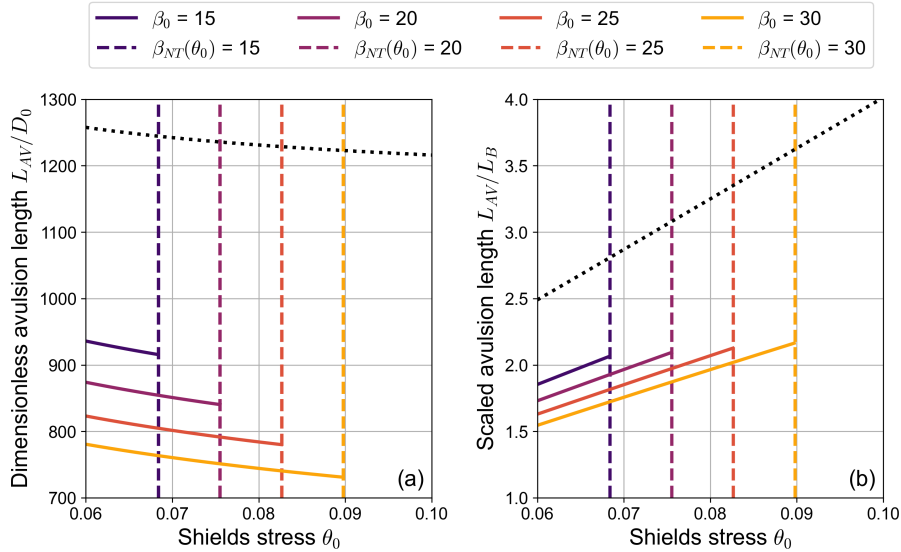


Figure AC2: Dependence of (a) the dimensionless avulsion length L_{AV}/D_0 and (b) the scaled avulsion length L_{AV}/L_B on the Shields stress θ_0 , as obtained from Equation (AC4). Vertical dashed lines indicate the value of Shields stress for which $\beta_0 = \beta_{NT}$, thus representing the boundary of the region of validity of the analytical model. The dotted line indicates the upper bound for L_{AV} , obtained by neglecting the β -dependent term $\Delta\eta_{BRT}$ ($C = 12$, transport formula by Meyer-Peter and Müller, 1948).

Dimensionless length falls in the range $L^* = 200 - 300$, which can be interpreted as a preferential range of length values that allows river loops to keep both branches active. The results reported in Figure AC2a suggest that these values are typically lower than the predicted dimensionless avulsion length L_{AV}/D_0 . We note, however, that the application of our model to this data-set is not straightforward, as the presence of the confluence may have an important influence on loop stability and equilibrium configuration (Ragno et al., 2021). Therefore, a direct comparison with our model's results would require incorporating the effect of the confluence, and considering the peculiar hydrodynamical and morphodynamical characteristics of individual field cases.

Regarding the estimate of the avulsion length proposed by the Reviewer based on Figure 9 of our paper, we observe that the figure does not include conditions of full avulsion, which would correspond to the intersection of the curves with the $\Delta Q = 1$ line (in-

cidentally, we also note that we define the aspect ratio β_0 as the half-width to depth ratio). To make this point clearer, we hereby provide the mathematical procedure, based on the analytical model described in Section 4 of our work, to compute the avulsion length L_{AV} as a function of the flow conditions in the upstream channel, namely the Shields stress θ_0 and the channel aspect ratio β_0 , provided the latter is larger than the no-transport aspect ratio β_{NT} . We'll also add the following paragraphs in the revised version of the manuscript.

The analytical model makes it possible to determine the marginal conditions for which one of the bifurcates closes completely (full avulsion), and to compute the associated avulsion length L_{AV} . This is accomplished by setting $D_c = 0$ in Equation (25a) of our paper, and isolating the length as:

$$L_{AV} = \frac{D_0}{S_0} \frac{1 - \frac{\Delta\eta_{BRT}}{2}}{1 - S_b/S_0}. \quad (\text{AC1})$$

The resulting expression highlights the key ingredients that determine the avulsion length, as all terms on the right-hand side of Equation (AC1) bring a precise physical meaning. Specifically, the first factor is the backwater length:

$$L_B = \frac{D_0}{S_0}, \quad (\text{AC2})$$

which provides the length scale of L_{AV} . Furthermore, the numerator of the second factor accounts for the aggradation experienced by the non-dominant branch until it stops transporting sediment, while the denominator holds the contribution of the incision of the dominant branch. The latter term can be determined from Equation (25b), by setting $\Delta Q = 1$ and using Equation (24), in the form:

$$\frac{S_b}{S_0} = \frac{1}{2} \left(\frac{S_b D_b}{S_0 D_0} \right)^{3/2} = \frac{1}{2} \left(\frac{\theta_b}{\theta_0} \right)^{3/2}. \quad (\text{AC3})$$

This allows us to re-write Equation (AC1) as

$$\frac{L_{AV}}{L_B} = \frac{1 - \frac{\Delta\eta_{BRT}}{2}}{1 - \frac{1}{2} \left(\frac{\theta_b}{\theta_0} \right)^{3/2}}, \quad (\text{AC4})$$

where θ_b can be calculated from mass conservation (Equation (23) of our paper).

Results reported in Figure AC2b reveal that the order of magnitude of L_{AV} is fixed by the backwater length. Moreover, as implied by Equation (AC4), the ratio L_{AV}/L_B increases with increasing Shields stress and decreases with increasing β_0 , due to the increase of the term $\Delta\eta_{BRT}$ (see Figure 10 of our paper).

2. The addition of the analytical model (25) is a noteworthy and helpful. But so that others can explore the model, I would suggest explicitly writing out the transport models that are used in the last component. The authors could also point towards what numerical method/tool they used to solve the system of nonlinear equations.

Results reported in our paper have been obtained using the transport relationship of Meyer-Peter and Müller (1948) and that of Parker (1978), as mentioned in Section 2. The adopted transport model is reported in the respective caption of each figure: we will include any missing information in the revised version of the manuscript.

To solve the nonlinear algebraic system, we simply use the default solver of the Python Scipy package. The solution seems to always converge, so we did not expect this choice to be critical.

3. Line 302: It is not clear to me what is meant by Beta_NT is calculated analytically. Is this arrived at by using the basic BRT analysis?

The Reviewer is right. The β_{NT} is calculated using the basic BRT analysis, as reported, for example, at the beginning of Section 3 (lines 231-232).

4. With reference to Fig 5. Why is there such an abrupt change (almost like a phase transition) at (or close to) Beta_NT. Is such a jump exhibited in the analytical model in (25)?

The abrupt change pointed by the Reviewer emerges from the results of the numerical simulations while gradually increasing β_0 from values smaller than the no-transport threshold β_{NT} to values larger than β_{NT} , as described in the first part of Section 3. Physically speaking, this abrupt change corresponds to a sharp transition in the system behaviour, as the non-dominant branch becomes unable to adapt its bedslope over time when its transport capacity vanishes. In this case, the BRT model is no longer applicable, as it assumes that both branches are morphodynamically active. This is why we developed a new analytical model (described in Section 4) to predict the long-term equilibrium state when $\beta_0 > \beta_{NT}$. Strictly

speaking, the analytical model defined by Equation (25) does not contain in itself any abrupt change. However, its applicability is obviously limited to cases where $\beta_0 > \beta_{NT}$.

References

- Bertoldi, W., & Tubino, M. (2007). River bifurcations: Experimental observations on equilibrium configurations. *Water Resources Research*, *43*(10), 1–10. <https://doi.org/10.1029/2007WR005907>
- Bolla Pittaluga, M., Repetto, R., & Tubino, M. (2003). Channel bifurcation in braided rivers: Equilibrium configurations and stability. *Water Resources Research*, *39*(3), 1–13. <https://doi.org/10.1029/2001WR001112>
- Meyer-Peter, E., & Müller, R. (1948). Formulas for Bed-Load transport. *IAHSR 2nd Meeting, Stockholm, Appendix 2*.
- Parker, G. (1978). Self-formed straight rivers with equilibrium banks and mobile bed. part 2. the gravel river. *Journal of Fluid Mechanics*, *89*, 127–146. <https://doi.org/10.1017/S0022112078002505>
- Ragno, N., Redolfi, M., & Tubino, M. (2021). Coupled Morphodynamics of River Bifurcations and Confluences [Publisher: Blackwell Publishing Ltd]. *Water Resources Research*, *57*(1). <https://doi.org/10.1029/2020WR028515>
- Ragno, N., Redolfi, M., & Tubino, M. (2022). Quasi-Universal Length Scale of River Anabranches. *Geophysical Research Letters*, *49*(16), e2022GL099928. <https://doi.org/10.1029/2022GL099928>
- Salter, G., Voller, V. R., & Paola, C. (2019). How does the downstream boundary affect avulsion dynamics in a laboratory bifurcation? [Publisher: Copernicus GmbH]. *Earth Surface Dynamics*, *7*(4), 911–927. <https://doi.org/10.5194/esurf-7-911-2019>
- Szewczyk, L., Grimaud, J.-L., & Cojan, I. (2020). Experimental evidence for bifurcation angles control on abandoned channel fill geometry [Publisher: Copernicus GmbH]. *Earth Surface Dynamics*, *8*(2), 275–288. <https://doi.org/10.5194/esurf-8-275-2020>